



Cite this: *Biomater. Sci.*, 2021, **9**, 4459

## Injectable *in situ* forming hydrogel gene depot to improve the therapeutic effect of STAT3 shRNA†

Da Yeon Kim, Hyeon Jin Ju, Jae Ho Kim, Sangdun Choi  and Moon Suk Kim  \*

Down-regulation of the signal transducer and activator of transcription 3 (Stat3) plays a crucial role in suppression of many solid tumors. Intratumoral injection of a gene carrier applying Stat3-small hairpin RNA (St3-shRNA) is a potential therapeutic strategy. To our knowledge, this is the first report of the intratumoral injection of St3-shRNA using a gene carrier. We herein designed biodegradable (methoxy)polyethylene glycol-*b*-(polycaprolactone-*ran*-polylactide) copolymer (MP) derivatized with a spermine group with cationic properties at the pendant position of the MP chain (MP-NH<sub>2</sub>). The designed MP-NH<sub>2</sub> can act as a gene carrier of St3-shRNA by forming an electrostatic complex with cationic spermine. This can increase the stability of the complexes because of protection of PEG in biologic environments and can exhibit a sol-gel phase transition around body temperature for the formation of intratumorally injected MP-NH<sub>2</sub> hydrogel depot for St3-shRNA. MP-NH<sub>2</sub> was observed to completely condense with St3-shRNA to form St3-shRNA/MP-NH<sub>2</sub> complexes. These complexes were protected for a relatively long time ( $\geq 72$  h) from external biologic molecules of the serum, DNase, and heparin. St3-shRNA/MP-NH<sub>2</sub> complexes in *in vitro* tumor cell experiments can enhance transfection of St3-shRNA, correspondingly enhance Stat3 knockdown efficiency, and inhibit tumor cell growth. St3-shRNA/MP-NH<sub>2</sub> complexes and St3-shRNA/MP-NH<sub>2</sub> complex-loaded hydrogel were intratumorally injected into the tumor as new efficient delivery carriers and depots of St3-shRNA. The intratumoral injection of St3-shRNA/MP-NH<sub>2</sub> complexes and St3-shRNA/MP-NH<sub>2</sub> complex-loaded hydrogel showed effective anti-tumor effect for an extended period of time due to the effect of Stat3 knockdown. Collectively, the development of MP-NH<sub>2</sub> as a carrier and depot of St3-shRNA provides a new strategy for St3-shRNA therapy through intratumoral injection with high efficacy and minimal adverse effects.

Received 20th April 2021,  
Accepted 8th May 2021

DOI: 10.1039/d1bm00624j  
[rsc.li/biomaterials-science](http://rsc.li/biomaterials-science)

## 1. Introduction

In most malignant tumors, the signal transducer and activator of transcription 3 (STAT3) is one of the cytoplasmic proteins involved in the malignant behaviors, such as tumor proliferation, metastasis, angiogenesis, survival, and immune evasion, and it is over-expressed in many malignant cancers, such as breast cancer, prostate cancer, and melanoma.<sup>1</sup> In addition, overexpression of STAT3 causes chemo-resistance.

Thus, down-regulation of STAT3 increases apoptosis in cancer cells and reduces cancer cell proliferation and survival. Several methods have been approached to down-regulate STAT3 using small molecule inhibitors for STAT3 function.<sup>2</sup> Among others, the use of small interfering RNA (siRNA) has

been proposed to suppress STAT3 function.<sup>3</sup> The purpose of such technology is to specifically induce the cleavage of STAT3 mRNA for efficient gene silencing.

The current siRNA utilization technology is designed to suppress the expression of specific genes in the cytoplasm and provide a new type of treatment with high target selectivity.<sup>4</sup> Various attempts including clinical trials have been made in this regard.<sup>5</sup> However, the main limitations of the therapeutic use of siRNA are rapid degradation in the cytoplasm and easy excretion from the kidney.<sup>6,7</sup>

Meanwhile, target gene expression can be also silenced using small hairpin RNA (shRNA), which has a tight hairpin rotational shape.<sup>8,9</sup> In addition, shRNA has relatively low rate of degradation and turnover. Furthermore, shRNA molecules have poor cell uptake and poor tissue specificity. Therefore, there is a need for an ideal vector for effective intracellular delivery of shRNA to increase cell uptake and prevent excretion from the desired site of action.<sup>10</sup>

The polyanionic nature of shRNA impairs cell uptake and limits its access to shRNA targets in the cell. To deliver shRNA to the desired site of action, its rapid degradation by

Department of Molecular Science and Technology, Ajou University, Suwon, 443-759, Korea. E-mail: [moonskim@ajou.ac.kr](mailto:moonskim@ajou.ac.kr); Fax: +82-31-219-3931; Tel: +82-31-219-2608  
† Electronic supplementary information (ESI) available. See DOI: [10.1039/d1bm00624j](https://doi.org/10.1039/d1bm00624j)

nucleases, absorption by reticuloendothelial system, and rapid kidney excretion must be overcome because all of these can remove shRNA early from biological systems. To address these hurdles, several delivery materials, including viral vectors, lipids, and polymer carriers, have been used in shRNA delivery studies.<sup>11–13</sup>

Nonetheless, viral vectors have high immunogenicity and unsatisfactory safety profiles, thus limiting the application of these delivery systems in clinical settings.<sup>14</sup> Conversely, cationic lipids and polymer carriers can be used to electrostatically bind negatively charged shRNAs to form effective complexes.<sup>15–17</sup> Furthermore, polymer carriers have the advantage of structural flexibility and can be chemically adjusted to obtain desirable physicochemical properties.

Among the cationic polymers, polyethylene imine (PEI) has a high cationic charge density and can thus effectively condense the polyanionic shRNA by electrostatic interaction between the anionic phosphate of the shRNA and the cationic amine of the PEI, thereby finally forming shRNA/PEI complexes.<sup>18</sup> Therefore, the formed shRNA/PEI complexes can be utilized in shRNA delivery studies.

Cationic polymers, including PEI, provide a platform for transporting shRNA by systemic administration, such as intravenous and intradermal injection, but only a small amount of shRNA is delivered to the tumor.<sup>19–21</sup> Therefore, multiple injections are often needed to maintain effective shRNA concentrations in tumor treatment. However, multiple injections lead to some concerns, such as reduced selectivity and facilitation of the reverse regulation process.<sup>22</sup> Conversely, it has been reported that direct intratumoral injection of an anticancer agent may provide appropriate local concentration of the anti-cancer agent in a targeted tumor.<sup>23–25</sup> Therefore, direct intratumoral injection of anticancer agents is a more potent and effective alternative with higher efficacy and fewer adverse effects when compared with systemic administration, such as intravenous and intradermal injection.

Recently, we reported the intratumoral delivery of anti-cancer drugs using *in situ* forming hydrogel drug carrier of biodegradable (methoxy)polyethylene glycol-*b*-(polycaprolactone-*ran*-polylactide) copolymer (MP).<sup>26,27</sup> The MP hydrogel showed a biodegradation half-life of 3 weeks and sol-gel phase transition at body temperature.

More recently, we prepared MP derivatized with methyl amine groups (MP-amine) at the pendant position on MP chains and examined their potential as biodegradable *in situ* forming hydrogel drug carriers.<sup>28–30</sup> The zeta potential of the MP-amine solution was 7–10 mV. In view of the above, it would be highly interesting to utilize MP-amine as a gene carrier through the formation of shRNA/MP-amine complexes by electrostatic interaction between anionic STAT3 shRNA (St3-shRNA) and cationic MP-amine. However, MP-amine in our previous work have a limited number of amines at the pendant position on MP chains. Thus, we considered a biodegradable MP derivatized with the spermine group (MP-NH<sub>2</sub>) with more cationic properties at the pendant position of the MP chain.

In this work, the designed MP-NH<sub>2</sub> comprised spermine cationic group for forming an electrostatic complex with St3-shRNA and a PEG group for increasing the stability of the complex under biologic environments. In addition, MP-NH<sub>2</sub> with PEG and polyester segments can exhibit a sol-gel phase transition at approximately 37 °C.

Thus, we aim to examine MP-NH<sub>2</sub> as a gene carrier of St3-shRNA through the formation of St3-shRNA/MP-NH<sub>2</sub> complexes and furthermore as an *in situ* forming hydrogel gene depot of St3-shRNA/MP-NH<sub>2</sub> complexes. To our knowledge, no previous studies have described the intratumoral injection of St3-shRNA/MP-NH<sub>2</sub> complexes and St3-shRNA/MP-NH<sub>2</sub> complex-loaded hydrogel gene depot to maximize the local tumor treatment effects at the intratumorally injected tumor site (Fig. 1). Therefore, the objectives of the current study were as follows: (1) to evaluate whether St3-shRNA/MP-NH<sub>2</sub> complexes can be tightly formed by electrostatic interaction between anionic St3-shRNA and cationic MP-NH<sub>2</sub> and whether they can be stably maintained under biologic molecules; (2) to examine whether the prepared St3-shRNA/MP-NH<sub>2</sub> complexes and St3-shRNA/MP-NH<sub>2</sub> complex-loaded hydrogel formulation can be intratumorally injected into the tumor to produce a gene depot of St3-shRNA; and (3) to determine whether the gene depot of St3-shRNA formed in the intratumorally injected tumor site holds the promise of achieving sustained action periods of Stat3 knockdown.

## 2. Materials and methods

### 2.1. Materials

Methoxy polyethylene glycol [MPEG, a number-average molecular weight ( $M_n$ ) = 750 g mol<sup>−1</sup>], stannous octoate, polyethylenimine (branched PEI, MW 10 kDa), dimethyl sulfoxide, acetic acid, and spermine were purchased from Sigma-Aldrich (St Louis, MO, USA). Glutaric anhydride was purchased from Acros Organics (Geel, Belgium). N-Hydroxysuccinimide (NHS), *N,N*-dicyclohexylcarbodiimide (DCC), and ε-caprolactone (CL) were purchased from TCI (Tokyo, Japan). CL was distilled over CaH<sub>2</sub> under reduced pressure. All other chemicals were of analytical grade and used without further purification.

### 2.2. Synthesis and characterization of MPEG-*b*-[polycaprolactone-*ran*-poly(spermine-*L*-lactide)] copolymer (MP-NH<sub>2</sub>)

All glasses were dried by hot heating in a vacuum and were flushed and handled under fresh dry nitrogen. 3-Benzylloxymethyl-6-methyl-1,4-dioxane-2,5-dione (LA-OBn) was prepared using a previously reported method.<sup>28</sup> For the preparation of the MP-OBn copolymer, MPEG (1.51 g, 2.02 mmol) in toluene (80 mL) was azeotropically distilled at 140 °C to completely remove water and then distilled off to give a final volume of toluene of 50 mL. Next, CL (3.79 g, 33.2 mmol) and LA-OBn (1.3 g, 5.2 mmol) were added, and then, 3 mL of a 0.1 M solution of stannous octoate in dried

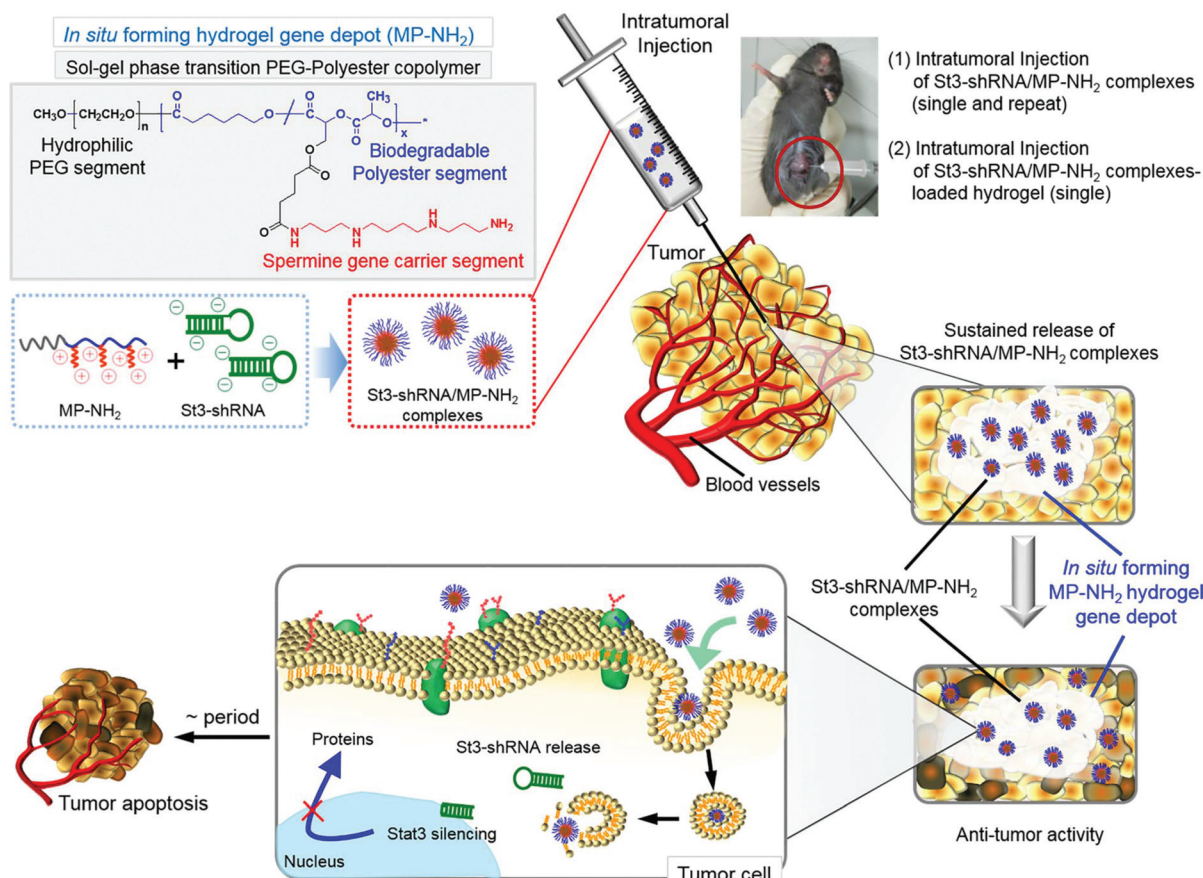


**Fig. 1** A schematic of tumor suppression via intratumoral injections of St3-shRNA/MP-NH<sub>2</sub> complexes or St3-shRNA/MP-NH<sub>2</sub> complex-loaded hydrogel gene depot (the image was created by D. Y. K. and M. S. K. using Adobe Photoshop 7.0 software).

toluene was added to the MPEG solution under a nitrogen atmosphere at room temperature. The reaction solution was polymerized for 24 h at 130 °C and then poured into a mixture of *n*-hexane and ethyl ether (v/v = 4/1) to precipitate the MP-OBn copolymer. The precipitated MP-OBn copolymer was filtered and dried in a vacuum, yielding 5.69 g (1.74 mmol, 86%) of colorless MP-OBn copolymer. The molecular weights of polycaprolactone (CL) and poly(benzyl-L-lactide) (PLA-OBn) segments in the MP-OBn copolymer were determined by <sup>1</sup>H-NMR spectrum. The proportions of PCL and PLA-OBn segments were respectively determined by comparing the total methylene protons in PCL at  $\delta$  = 2.3 ppm and the phenyl proton signals of PLA-OBn at  $\delta$  = 7.2–7.4 ppm with the total methyl protons in MPEG at  $\delta$  = 3.38 ppm as a standard of 750 g mol<sup>-1</sup>.

For preparation of MP-OH, the MP-OBn copolymer (1.6 g, 0.49 mmol) was dissolved in anhydrous THF (50 mL). Then, the 10% w/w (1 g) of Pd/C [palladium, 10 wt% (dry basis) on activated carbon (50% water w/w, Degussa type E101 NE/W)] was added to the MP-OBn copolymer solution. The suspension was stirred under a hydrogen atmosphere for 12 h. The reaction suspension was filtered using a Celite filter to remove the reaction catalyst. The solution was concentrated by rotary evap-

oration and dried in a vacuum, yielding 1.2 g (0.41 mmol, 84%) of colorless MP-OH copolymer.

Next, MP-OH (1.2 g, 0.41 mmol) in toluene (80 mL) was azeotropically distilled for 4 h at 140 °C to completely remove water and was then distilled off to give a final toluene volume of 30 mL. Glutaric anhydride (0.61 g, 5.3 mmol) in the presence of acetic acid (1.2 mL) was added to the MC-OH solution. The reaction solution was stirred at 100 °C for 24 h and then poured into a mixture of *n*-hexane and ethyl ether (v/v = 1/1) to precipitate an MP-COOH copolymer. The precipitated copolymer was dried in a vacuum to give a colorless MP-COOH copolymer (1.1 g, 0.28 mmol, 68%).

Finally, for the preparation of MP-NH<sub>2</sub>, MP-COOH (0.6 g, 0.15 mmol) was dissolved in DMSO (30 mL). Then, DCC (37.2 mg, 0.18 mmol) and NHS (20.7 mg, 0.18 mmol) were added into the MP-COOH solution and stirred for 3 h. Spermine (40 mg, 0.19 mmol) was then added to the reaction solution which was stirred for 3 h at room temperature.

The reaction solution was poured into a dialysis tube (molecular weight cut-off: 3.5 kDa, Spectrum Laboratories, CA, USA) and dialyzed for 2 days to remove unreacted DCC and NHS; then, it was freeze-dried at -70 °C for 3 days to finally give MP-NH<sub>2</sub>. The elemental analysis of the calculated values for

MP-NH<sub>2</sub> was as follows: C: 60.8, H: 7.2, and N: 6.1. In addition, the measured values were as follows: C: 56.26, H: 8.56, and N: 3.19. MP-NH<sub>2</sub> was sterilized using UV for following experiment because amine on MP-NH<sub>2</sub> can react with ethylene oxide.

### 2.3. Preparation of STAT3 shRNA (St3-shRNA)

The St3-shRNA plasmid (pGFP-V-RS vector containing the 29-mer shRNA sequence ACCTGAAGACCAAGTCATCTGT-GTGACA, ID: GI556360) was obtained from OriGene Technologies (Rockville, MD), electroporated into *Escherichia coli* (*E. coli* strain XL1-Blue), amplified in LB agar plate (with 50 µg mL<sup>-1</sup> kanamycin) for 1 day, and then transformed to LB media (with 50 µg mL<sup>-1</sup> kanamycin), followed by culturing for 17 h. St3-shRNA was purified by PureLink™ HiPure Plasmid Filter Midiprep Kit according to the manufacturer's protocol (Invitrogen, Löhne, Germany). The quantity and purity were determined using ND-1000 spectrophotometer (NanoDrop Technologies; Wilmington, DE, USA).

### 2.4. Monitoring complexes formation by agarose gel electrophoresis

St3-shRNA/MP-NH<sub>2</sub> or St3-shRNA/PEI complexes (containing 10 µg St3-shRNA) with the N/P charge ratio from 0 to 128 were prepared in DW (20 µL) and stabilized for 30 min. The complexes were visualized on 1.2% agarose gel loaded with 10 µg ethidium bromide (EtBr; Amresco, OH, USA) using UVP (BioDoc-It™ Imaging System, CA, USA).

### 2.5. Zeta potential and particle sizes

The zeta potentials and particle sizes of St3-shRNA/MP-NH<sub>2</sub> or St3-shRNA/PEI complexes with the N/P charge ratio from 0 to 128 were measured by dynamic light scattering (DLS, ELSZ-1000; Otsuka Electronics, Osaka, Japan). All zeta potentials were measured by scanning three times and were repeated four times.

### 2.6. Atomic force microscopy

The AFM images for St3-shRNA alone, MP-NH<sub>2</sub> alone, St3-shRNA/MP-NH<sub>2</sub>, and St3-shRNA/PEI complexes were individually transferred onto a washed silicon wafer with MeOH. The wafer was quickly placed in liquid nitrogen and freeze dried for a day. AFM measurements were carried out in the non-contact mode AFM (XE-100 AFM, Park system, Suwon, Korea).

### 2.7. DNase and serum protection of St3-shRNA

The naked St3-shRNA, St3-shRNA/MP-NH<sub>2</sub>, and St3-shRNA/PEI complexes with the N/P charge ratio of 16 were incubated in the presence of serum or DNase I (Sigma, MO, USA) to confirm the protection of St3-shRNA/MP-NH<sub>2</sub> or St3-shRNA/PEI complexes. Then, 7.5 µL FBS (final concentration 25% v/v) or DNase (100 µg) and 2.5 µL loading dye (1 µL of 10× Blue Juice, Invitrogen, CA, USA) were added into 20 µL of complexes. Aliquots of 30 µL were taken at 30 min, 1, 3, 5, 12, 24, 48, 60, 72, and 84 h, and 2 µL of 200 mg mL<sup>-1</sup> heparin sodium (Acros organics, NJ, USA) was immediately added to decomplex St3-shRNA from St3-shRNA/MP-NH<sub>2</sub> or St3-shRNA/PEI com-

plexes and incubated for 15 min. The complexes were visualized on 1.2% agarose gel loaded with 10 µg EtBr using UVP. The analysis of the agarose gel areas including the bands at each point was performed to analyze their residual ratio. The value for time 0 min was set at 100% to normalize the amount of residual naked St3-shRNA.

### 2.8. Heparin stability assay of St3-shRNA

St3-shRNA/MP-NH<sub>2</sub> or St3-shRNA/PEI complexes were prepared as described in previous section. Then, 1, 2.5, 5, 10, 25, 50, 75, 100, and 200 µg of heparin sodium was added to St3-shRNA/MP-NH<sub>2</sub> or St3-shRNA/PEI complexes and incubated for 15 min at room temperature. The complexes were then visualized on 1.2% agarose gel loaded with 10 µg EtBr using UVP.

### 2.9. *In vitro* antitumor activity

B16F10 cancer cells were cultured in 75 cm<sup>2</sup> tissue culture flask (BD Falcon; San Jose, CA, USA) in α-minimal essential medium (α-MEM; Gibco; NY, USA) prepared with 10% fetal bovine serum (FBS; Gibco; NY, USA) and 1% penicillin-streptomycin (PS; Gibco; NY, USA) in 5% CO<sub>2</sub> at 37 °C.

St3-shRNA/MP-NH<sub>2</sub> or St3-shRNA/PEI complexes with the N/P charge ratio of 1–64 were prepared. The complexes were added into B16F10 melanoma cells (2 × 10<sup>4</sup> cells per well) seeded in a 24-well plate and were then incubated for 4 h. The cells were then washed with serum free MEM and replaced in fresh culture medium.

After 24, 48, and 72 h, the *in vitro* cytotoxicity of all complexes toward B16F10 cancer cells was compared using the MTT assay [3-(4,5-dimethylthiazol-2-yl)-2,5-diphenyltetrazolium bromide; Sigma-Aldrich Co., St Louis, MO, USA]. In brief, 100 µL of PBS solution containing the MTT tetrazolium substrate (50 µg mL<sup>-1</sup>) was added to each 96-well plate, and the plates were incubated at 37 °C for 4 h. The resulting violet formazan precipitate was solubilized by adding 500 µL of DMSO and shaken for 30 min. The solutions were placed in 96-well plates and read using an ELISA plate reader (EL808 ultra microplate reader; Bio-Tek Instruments, VT, USA). The optical density of each well was measured at a wavelength of 590 nm. All experiments were performed at least three times, and the results were presented as mean ± standard deviation (SD).

### 2.10. Transfection of B16F10 cancer cells

B16F10 cancer cells were seeded in 24-well plates at a density of 2 × 10<sup>4</sup> cells per well and incubated for 24 h before transfection. Then, 1 µg of St3-shRNA was added to each well in the form of St3-shRNA/MP-NH<sub>2</sub> or St3-shRNA/PEI complexes with the N/P charge ratio ranging from 1 to 64 with triplicate wells per condition.

Each B16F10 was washed with serum-free MEM and incubated with St3-shRNA/MP-NH<sub>2</sub> or St3-shRNA/PEI complexes for 4 h, and then, it was washed with serum-free MEM and placed in fresh culture medium. At 24 h, 48 h and 72 h, 1 µg mL<sup>-1</sup> of Hoechst 33342 (Invitrogen, Carlsbad, CA, USA) was added to the plate for staining nucleic acids (blue). Images

showing blue fluorescence in B16F10 cancer cells were observed using fluorescence microscopy (Axio Imager A1, Carl Zeiss Microimaging GmbH; Gottingen, Germany). GFP-expressing cells were detected using a FACSCanto II flow cytometer (BD Biosciences, CA, USA) with 520 nm and 570 nm bandpass filters for GFP. Approximately 10 000 events were acquired per sample, and data analysis was performed using WinMDI software.

### 2.11. *In vivo* antitumor activity

The protocols of this study were approved by the Institutional Animal Experiment Committee (approval no. 2012-0019) of the School of Medicine, Ajou University. The *in vivo* experiments were carried out in accordance with the approved guidelines by the Animal Ethics Committee for Care and Use of Laboratory Animal Research Center of Ajou University Medical Center. The tumor model was established by subcutaneous inoculation of approximately  $2 \times 10^5$  B16F10 melanoma cells (in a 100  $\mu$ L suspension) into the abdomen of C57BL/6 mice (6-weeks-old, female, 17–20 g). The time at which the volume of the solid tumors reached  $165 \pm 14$  mm<sup>3</sup> was defined as day 0.

St3-shRNA/MP-NH<sub>2</sub> (St3-shRNA, 50  $\mu$ g) with the N/P charge ratio of 16 was prepared in 100  $\mu$ L of DW. An MP-NH<sub>2</sub> solution was prepared at 20 w/v% in DW. St3-shRNA/MP-NH<sub>2</sub> (St3-shRNA, 50  $\mu$ g) was added to 100  $\mu$ L of 20 w/v% MP-NH<sub>2</sub> as intratumoral injection formulation (St3-shRNA/MP-NH<sub>2</sub> complex-loaded hydrogel).

The animals were randomly divided and assigned to four experimental groups: (1) normal saline, (2) single injection of St3-shRNA/MP-NH<sub>2</sub> complexes (St3-shRNA, 50  $\mu$ g per mouse), (3) repeat injection of St3-shRNA/MP-NH<sub>2</sub> complexes (St3-shRNA, 50  $\mu$ g per mouse at each injection) at 3, 6, 9, 12, and 15 days, and (4) single injection of St3-shRNA/MP-NH<sub>2</sub> complex-loaded hydrogel formulation (St3-shRNA, 50  $\mu$ g). On day 0, 100  $\mu$ L of each formulation was intratumorally injected into the tumor using a 21-gauge needle on a disposable 1 mL syringe. Antitumor activity was assessed by measuring tumor diameters in two dimensions with Vernier calipers on predefined days. The tumor volume ( $V$ ) was calculated according to the following formula:  $V = [\text{length} \times (\text{width})^2]/2$ .

On days 1, 7, and 16 after injection, mice were euthanized, and tumors were individually dissected and removed from the subcutaneous area of the abdomen. Tumor tissue samples were immediately fixed with 10% formalin.

### 2.12. Determination of the expression of the STAT3

RNA was isolated from the excised tumor tissue with TRIzol solution (Invitrogen; CA, USA). RNA was quantified using an ND-1000 spectrophotometer (NanoDrop Technologies; Wilmington, DE, USA) at 260 nm, and the concentration and quality were confirmed using agarose gel electrophoresis. The removed RNA (50 ng) was then reverse-transcribed to cDNA using SuperScript Double-Stranded cDNA Synthesis Kit (Invitrogen, CA, USA). PCR amplification and real-time fluorescence detection of STAT3 and GAPD were performed with a

Chromo4 Real-Time PCR System (Bio-Rad; Hercules, CA, USA) using Power SYBR® Green (Applied Biosystems; UK). The expression of the STAT3 was normalized to GAPDH expression. All samples were analyzed in triplicate. Data analysis was conducted using the comparative cycle threshold (Ct) method ( $2^{-\Delta\Delta\text{Ct}}$ ) for relative quantification. The PCR primers (GenoTech, Daejeon, Korea) used were as follows: STAT3 primer (forward: 5'-CATGGCTATAAGATCATGGATGCGAC-3', reverse: 5'-AGGGCTCAGCACCTTCACCGTTATTTC-3') and GAPDH (forward: 5'-CAAGGTATCCATGACAACTTG-3', reverse: 5'-GTCCACCAC-CCTGTTGCTGTAG-3').

### 2.13. Histological analysis

On days 1, 7, and 16 after injection, mice were sacrificed, and the tumors were individually dissected and removed from the subcutaneous area of the abdomen. In each staining, tissues were extracted from one animal at each pre-designed experimental time, made into three or more slides and then stained. The slides of each staining were evaluated in independent experimental groups with  $n = 3$  for each data point. The tumor tissue samples were immediately fixed with 10% formalin and embedded in paraffin. The embedded specimens were sectioned (4  $\mu$ m) along the longitudinal axis of the tumor and incubated at 70 °C for 2 h to remove the paraffin. The slides were deparaffinized twice with xylene and then hydrated using 100, 95, 70, and 60% ethyl alcohol in series. For hematoxylin and eosin (H&E) staining, the samples were washed in running DW and stained with hematoxylin and eosin for 3 min each. Thereafter, the stained slides were fixed and mounted with a mounting medium (Muto Pure Chemicals, Tokyo, Japan).

Apoptotic cells were identified using a terminal transferase dUTP nick-end labeling (TUNEL) assay kit (*In situ* cell death detection kit, TMR red, Roche, Germany) following the manufacturer's protocol. Briefly, the slides were deparaffinized at 70 °C, hydrated, and washed three times with PBS-T (0.1% Tween-20 in PBS) for 10 min. The tissue samples were incubated with 1 mg mL<sup>-1</sup> proteinase K (Invitrogen, Carlsbad, CA, USA) in TE buffer at 37 °C for 20 min and washed with PBS-T (0.1% Tween-20 in PBS). The tissues were incubated with 0.1% Triton X-100 at 4 °C for 5 min and treated with a mixture of label solution and enzyme solution (9 : 1) at 37 °C for 60 min. The slides were counterstained with 4',6-diamidino-2-phenylindole (DAPI) and mounted with fluorescent mounting solution (DaKo, Glostrup, Denmark). Immunofluorescent images were obtained using an Axio Imager A1 and analyzed with Axiovision Rel. 4.8 software.

For CD31 staining, the slides were hydrated for 5 min and treated with citrate buffer solution at 120 °C–130 °C for 10 min. The slides were washed with PBS and PBS-T (0.05% Tween-20 in PBS) and blocked with 5% bovine serum albumin (BSA; Millipore, Billerica, MA, USA) and 5% horse serum (HS, Gibco, Auckland, New Zealand) in PBS for 90 min at 37 °C. The sections were incubated for 16 h at 4 °C with CD31 antibodies (rabbit anti-mouse CD31; Abcam, Cambridge, UK) diluted in antibody diluent (DaKo, Glostrup, Denmark) (1 : 200); then, they were washed with PBS and PBS-T and incu-

bated with secondary antibodies (rat anti-mouse Alexa Fluor594; Invitrogen, Carlsbad, CA, USA) for 3 h at room temperature in the dark. The slides were washed with PBS and PBS-T, counterstained with DAPI in DW (1 : 1000) for 20 min, and mounted with fluorescent mounting solution (Dako, Glostrup, Denmark).

#### 2.14. Statistical analysis

All data of zeta potential, particle size, cytotoxicity, transfection, STAT3 expression, TUNEL assay, and CD31 assay were obtained from independent experiments in which each treatment condition was tested in triplicate. Tumor sizes were evaluated in independent experimental groups with  $n = 3$  for each data point. All data are presented as mean  $\pm$  SD. The results were analyzed by one-way ANOVA with Bonferroni's multiple comparisons test. Statistical analyses were performed with SPSS 12.0 software (IBM Corporation, Armonk, NY, USA).

### 3. Results and discussion

#### 3.1. Preparation of MP-NH<sub>2</sub> gene carrier

Amine group is one of the most useful carrier available for gene delivery. We previously reported the preparation and

characterization of the MP-amine copolymers.<sup>28</sup> In this work, spermine was selected for preparing the pendant amine group-functionalized MP-NH<sub>2</sub> copolymer.

The molecular weight and the PCL/PLLA ratio of the prepared MP-NH<sub>2</sub> diblock copolymer were 3000 g mol<sup>-1</sup> and 87/13, respectively. The structure of MP-NH<sub>2</sub> was fully confirmed by <sup>1</sup>H-NMR and elemental analysis (Fig. 2). The spermine content of MP-NH<sub>2</sub> was 60% of the target value.

MP-COOH (precursor) solution exhibited a negative zeta potential of -32.4 mV, whereas MP-NH<sub>2</sub> solution exhibited a positive zeta potential of 20.6 mV. These results indicated that the pendant spermine group-functionalized MP-NH<sub>2</sub> with positive zeta potential was successfully prepared as a gene carrier.

Thus far, one of the most widely studied *in situ* forming hydrogels prepared are amphiphilic copolymers containing both hydrophilic and hydrophobic segments.<sup>31</sup> MP-NH<sub>2</sub> is also an amphiphilic copolymer as it contains hydrophilic PEG and a hydrophobic PCL/PLLA segment. In previous works, several groups examined the *in vitro* and *in vivo* biodegradation of similar polymers with MP-NH<sub>2</sub>.<sup>32-39</sup> We observed the degraded oligomers including PEG, lactic acid with carboxylic acid group and hexanolic acid. We believed that the degraded products have no/little significant systemic effect on our body.

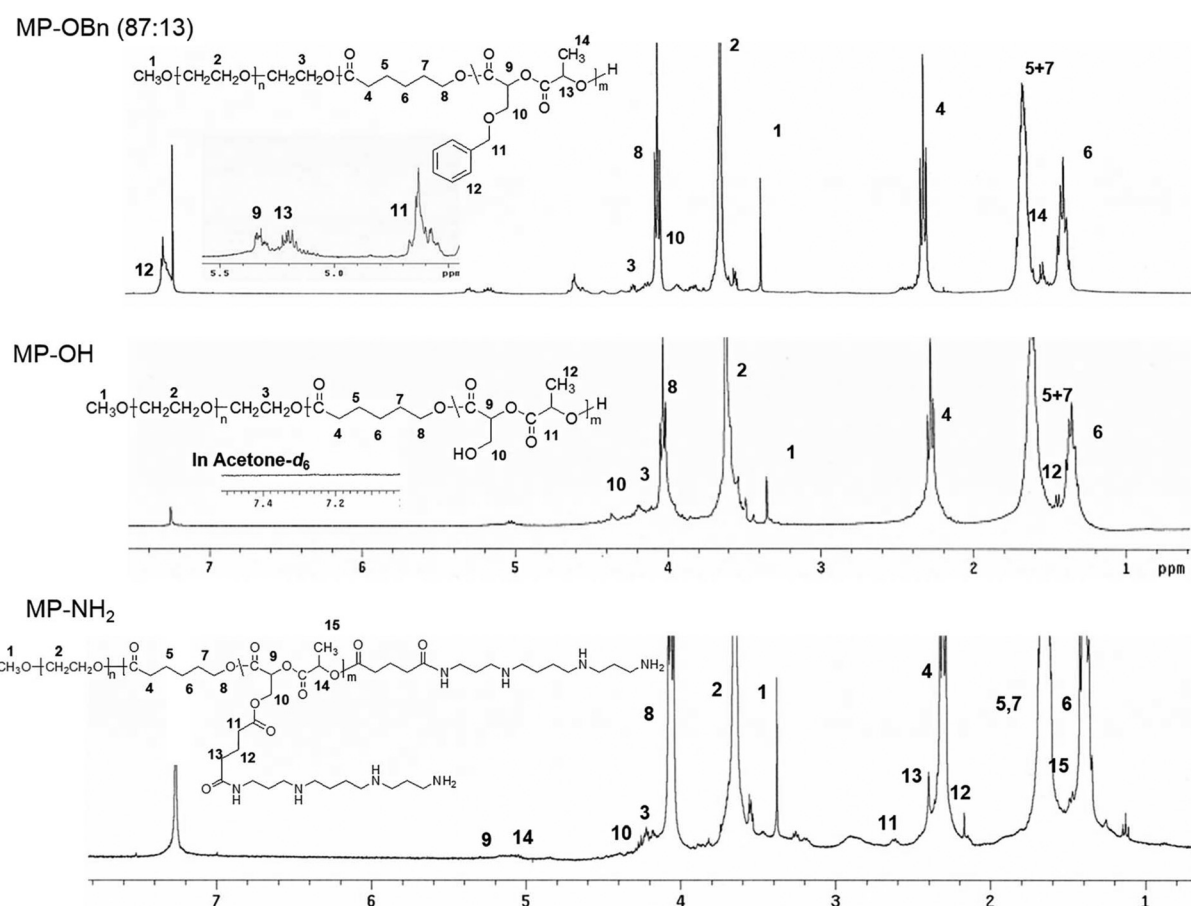


Fig. 2 <sup>1</sup>H NMR spectra of precursor MP-OBn, MP-OH and MP-NH<sub>2</sub>.

Thus, to examine the feasibility of MP-NH<sub>2</sub> as *in situ* forming hydrogel gene, the phase transition of MP-NH<sub>2</sub> was examined by visually inspecting gelation at different temperatures between 25 °C and 37 °C. MP-NH<sub>2</sub> solutions flowed at 25 °C, whereas MP-NH<sub>2</sub> did not flow at 37 °C when tilted. MP-NH<sub>2</sub> exhibited distinct sol-gel phase transition at 37 °C. The phase transition was induced by intra- and inter-hydrophobic interactions of hydrophobic PCL/PLLA segments.<sup>26,27</sup> These results indicated that the sol-gel phase transition of MP-NH<sub>2</sub> can be used as an *in situ* forming hydrogel gene depot through intratumoral injection.

### 3.2. Preparation and characterization of St3-shRNA/MP-NH<sub>2</sub> complexes

For gene delivery, the formation of gene complexes *via* electrostatic interaction is an important prerequisite.<sup>11–13</sup> MP-NH<sub>2</sub> with a positive zeta potential due to the spermine group was a good candidate for the electrostatic interaction with St3-shRNA.

Thus, to examine the feasibility of MP-NH<sub>2</sub> as a gene carrier, St3-shRNA/MP-NH<sub>2</sub> complexes were formed by mixing MP-NH<sub>2</sub> and St3-shRNA solutions according to the varying N/P charge ratios. For comparison, St3-shRNA/PEI complexes were also formed using PEI and St3-shRNA with varying N/P charge ratios.

Agarose gel electrophoresis was performed and fluorescence measurements were taken to identify the optimal charge ratio at which St3-shRNA is fully bound to MP-NH<sub>2</sub> or PEI. EtBr fluoresces when intercalated into free St3-shRNA, but the fluorescence intensity decreased as St3-shRNA was bound to MP-NH<sub>2</sub> or PEI (Fig. 3a). We found that St3-shRNA and MP-NH<sub>2</sub> condensation was complete at N/P charge ratios greater than 8, as shown by the loss of EtBr at higher N/P ratios. Meanwhile, St3-shRNA and PEI were completely complexed at an N/P charge ratio of 2.

Fig. 3b shows the surface charge of St3-shRNA/MP-NH<sub>2</sub> and St3-shRNA/PEI complexes at N/P charge ratios of 1–128. St3-shRNA alone exhibited a surface charge of -31 mV, as measured by DLS. St3-shRNA/MP-NH<sub>2</sub> complexes formed at N/P charge ratios of 1, 2, and 4 exhibited negative charges of -27 mV, -20 mV, and -8 mV, respectively. At the N/P charge ratio of 8, St3-shRNA/MP-NH<sub>2</sub> complexes exhibited a positive charge of 2.3 mV. Thereafter, the surface charge value gradually increased with increasing N/P charge ratios and became 31 mV at the N/P charge ratio of 128. This indicated that the negative surface charge of St3-shRNA was converted to a net positive surface charge by the addition of MP-NH<sub>2</sub> to form St3-shRNA/MP-NH<sub>2</sub> complexes.

Meanwhile, St3-shRNA/PEI complexes formed at N/P charge ratios of 1 and 2 showed negative charges of -20 mV and -12 mV, respectively, even though the formation of St3-shRNA/PEI complexes was complete at N/P charge ratios of 1 and 2, as shown by gel electrophoresis and fluorescence (Fig. 3a). At the N/P charge ratio of 4, St3-shRNA/PEI complexes exhibited a positive charge of 1 mV, and this value gradually increased up to 52 mV with increasing N/P charge ratios.

DLS measurements indicated that the diameter of St3-shRNA/PEI complexes ranged from 330 nm to 150 nm and decreased as the concentration of PEI increased (Fig. 3c). Meanwhile, St3-shRNA/MP-NH<sub>2</sub> complexes showed diameters of 760 nm, 524 nm, 330 nm, and 240 nm at N/P charge ratios of 1, 2, 4, and 8, respectively. From the N/P charge ratio of 16, two complexes were observed. The diameter of one complex gradually decreased up to 150 nm with increasing N/P charge ratios, whereas that of the other one increased up to 1770 nm with increasing N/P charge ratios. It was conjectured that a small diameter was assignable to the complexes of St3-shRNA completely condensed with MP-NH<sub>2</sub> and that a large diameter was assignable to the micelle formation of excess MP-NH<sub>2</sub>, because MP-NH<sub>2</sub> has already been formed the complexes with small amounts of St3-shRNA.

The structure and morphology of St3-shRNA/MP-NH<sub>2</sub> and St3-shRNA/PEI complexes were observed by AFM. St3-shRNA showed thread-like appearance. MP-NH<sub>2</sub> alone exhibited complexed form of 987 nm size, indicating micelle formation.

St3-shRNA/MP-NH<sub>2</sub> complexes formed at N/P charge ratios of 4 were almost spherical with a diameter of 333 nm. The complexes at N/P charge ratios of 16 were spherical with small and large sizes representing St3-shRNA/MP-NH<sub>2</sub> complexes and MP-NH<sub>2</sub> micelle, respectively. The AFM and DLS results were in good agreement. These results indicated that MP-NH<sub>2</sub> efficiently condensed with St3-shRNA to generate St3-shRNA/MP-NH<sub>2</sub> complexes of varying N/P ratios, even though excess MP-NH<sub>2</sub> formed micelles.

These results suggest that when a mixture of a small amount of St3-shRNA and a relative large amount of MP-NH<sub>2</sub> is prepared as an injectable *in situ* forming hydrogel formulation, St3-shRNA/MP-NH<sub>2</sub> complexes form, and they can be included inside injectable *in situ* forming hydrogel which mean gene depot of St3-shRNA.

Generally, PEG has low toxicity and is unlikely to have specific interactions with biological molecules; therefore, it can protect activation by biological signals.<sup>40</sup> The designed MP-NH<sub>2</sub> can increase the stability of complexes by PEG in biologic environments.

To confirm the stability of St3-shRNA under biologic molecules, naked St3-shRNA, St3-shRNA/PEI, and St3-shRNA/MP-NH<sub>2</sub> complexes were incubated with serum, DNase, and heparin (Fig. 4). The stability of St3-shRNA was confirmed by gel electrophoresis, and then, the amount of each St3-shRNA was determined based on the intensity of gel electrophoresis images.

The naked St3-shRNA had disappeared within 12 h in the serum and 24 h in DNase, indicating degradation of St3-shRNA. In contrast, the retention time of St3-shRNA from St3-shRNA/PEI and St3-shRNA/MP-NH<sub>2</sub> complexes increased to ≥72 h in serum and DNase. St3-shRNA/MP-NH<sub>2</sub> complexes showed that 90% St3-shRNA remained at 12 h, 80% at 24 h, and 38% of after 72 h. In addition, it was confirmed that St3-shRNA/MP-NH<sub>2</sub> complexes had a retention stability 1.5 times or higher than that of St3-shRNA/PEI in serum or DNase.

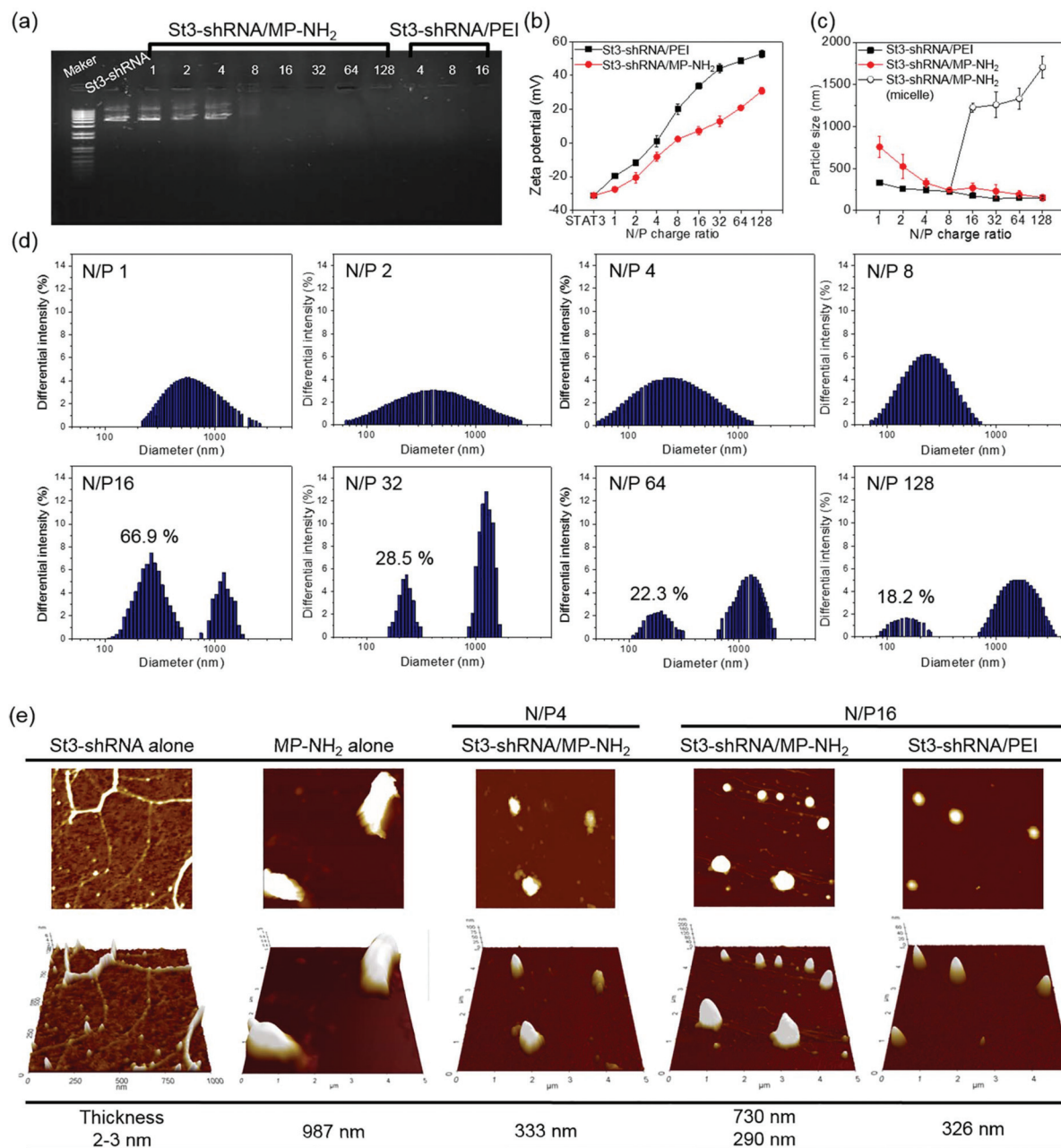


**Fig. 3** (a) Agarose gel electrophoresis of St3-shRNA/MP-NH<sub>2</sub> and St3-shRNA/PEI complexes at various N/P charge ratios. (b) zeta potential, (c) particle size, and (d) size distribution of St3-shRNA/MP-NH<sub>2</sub> and St3-shRNA/PEI complexes determined by dynamic light scattering and (e) AFM images of naked St3-shRNA, MP-NH<sub>2</sub> alone, St3-shRNA/PEI, and St3-shRNA/MP-NH<sub>2</sub> complexes with N/P charge ratios of 4 and 16.

Furthermore, to evaluate the stability of shRNA/PEI and St3-shRNA/MP-NH<sub>2</sub> complexes in the presence of heparin, the stability of shRNA/PEI and St3-shRNA/MP-NH<sub>2</sub> was evaluated by treating them with various concentrations of heparin.

St3-shRNA remained protected when exposed to low concentrations of heparin but was completely dissociated and released from shRNA/PEI and St3-shRNA/MP-NH<sub>2</sub> when treated with a high concentration of heparin (200 µg). Only 20% of St3-shRNA/PEI complexes remained protected in

100 µg heparin, whereas St3-shRNA/MP-NH<sub>2</sub> complexes remained protected more than 63% under the same condition. In addition, it was confirmed that St3-shRNA/MP-NH<sub>2</sub> complexes had 2–3 times more stability than St3-shRNA/PEI complexes when treated with heparin.

Collectively, it was conjectured that St3-shRNA forms St3-shRNA/MP-NH<sub>2</sub> complexes more efficiently with MP-NH<sub>2</sub>. The PEG chain of the formed St3-shRNA/MP-NH<sub>2</sub> complexes protected from external biologic molecules of serum, DNase or heparin for a relatively long time.

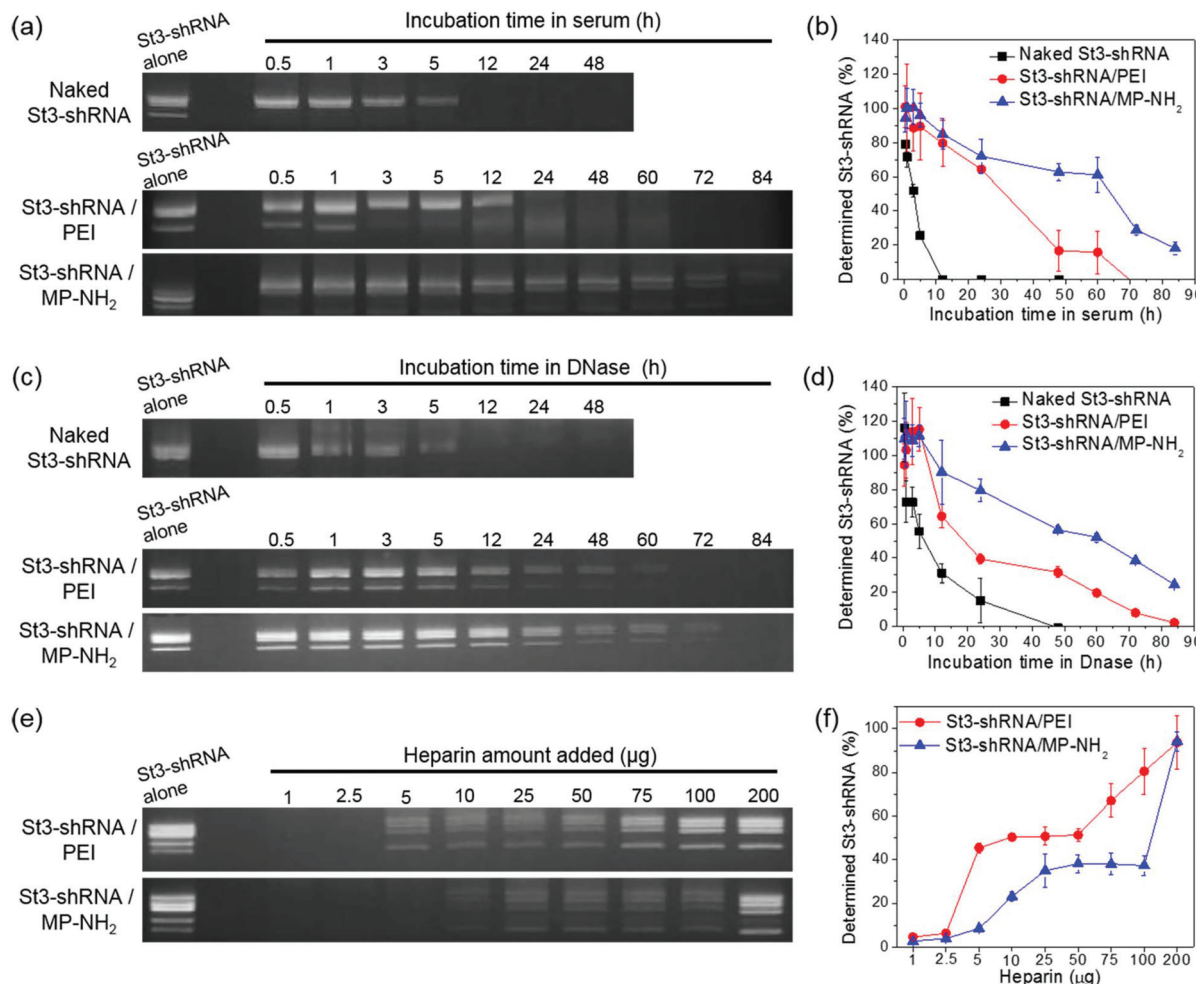


**Fig. 4** Timed change profile of naked and complexed St3-shRNA: (a and c) the gel results for naked St3-shRNA, St3-shRNA/PEI, and St3-shRNA/MP-NH<sub>2</sub> complexes (with the N/P charge ratio of 16) after incubation in (a and b) 25% serum and (c and d) 100 µg DNase and (b and d) the percentage of intact St3-shRNA recovered from different complexes. Heparin stability assay of complexed St3-shRNA/PEI and St3-shRNA/MP-NH<sub>2</sub>: (e) the gel results for St3-shRNA/PEI and St3-shRNA/MP-NH<sub>2</sub> complexes after incubation in heparin and (f) the percentage of intact St3-shRNA recovered from St3-shRNA/PEI and St3-shRNA/MP-NH<sub>2</sub> complexes.

### 3.3. Cytotoxicity of St3-shRNA/MP-NH<sub>2</sub> complexes

To determine whether MP-NH<sub>2</sub> and PEI were cytotoxic to B16F10 cells when present in complexes, the cells were incubated for 72 h with St3-shRNA/PEI and St3-shRNA/MP-NH<sub>2</sub> complexes at different N/P charge ratios, and their viabilities were then measured by the MTT assay. The optical density (directly proportional to viability) of B16F10 cells was determined at 24 h, 48 h, and 72 h after incubation with St3-shRNA/PEI and St3-shRNA/MP-NH<sub>2</sub> complexes (Fig. 5). Compared with control cells, St3-shRNA/PEI complexes showed 33% cytotoxicity even at the N/P charge ratio of 1. Cytotoxicity gradually increased at N/P charge ratios of 2–16 and was 70% and 85% at N/P charge ratios of 32 and 64, respectively, indicating rapidly increased cytotoxicity of PEI against B16F10 cells. These data demonstrate that cytotoxicity against B16F10 cells was proportional to the N/P charge ratio of St3-shRNA/PEI complexes.

Meanwhile, St3-shRNA/MP-NH<sub>2</sub> complexes showed 13%–16% cytotoxicity at N/P charge ratios of 1–3 and 30%–34%

cytotoxicity at N/P charge ratios of 8–64. In addition, cytotoxicity of St3-shRNA/MP-NH<sub>2</sub> complexes was four times less than that of St3-shRNA/PEI. These data show that MP-NH<sub>2</sub> showed little cytotoxicity compared with PEI.

### 3.4. Transfection efficiency of St3-shRNA

St3-shRNA used encoded the fluorescent GFP protein, which allowed for transfection efficiency to be assessed by GFP fluorescence imaging of cells. For this purpose, naked St3-shRNA was added to B16F10 cancer cells, and transfection efficiencies were examined. No GFP expression was observed in B16F10 cancer cells transfected with naked St3-shRNA. In contrast, St3-shRNA/PEI and St3-shRNA/MP-NH<sub>2</sub> complexes showed fluorescence emanating from B16F10 cells, indicating the transfection of B16F10 cells (Fig. 6a and b).

Next, the transfection efficiency of St3-shRNA/PEI and St3-shRNA/MP-NH<sub>2</sub> complexes was quantified by flow cytometry (Fig. 6c and d). St3-shRNA/PEI and St3-shRNA/MP-NH<sub>2</sub> showed

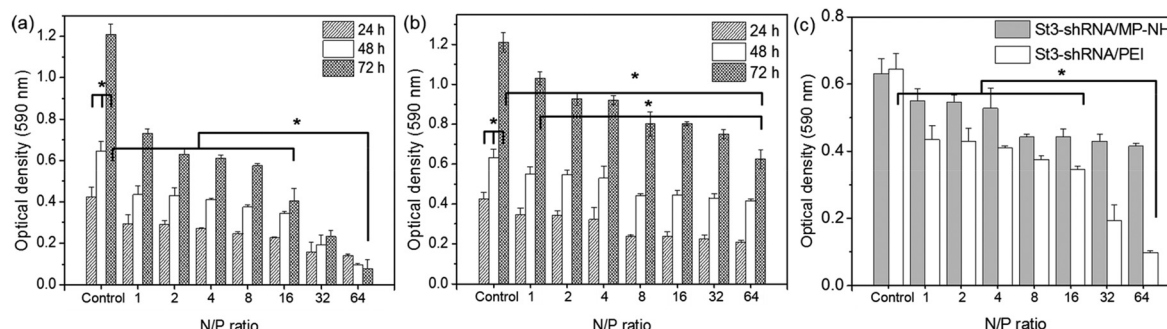


**Fig. 5** Cytotoxicity assay of (a) St3-shRNA/PEI complexes, (b) St3-shRNA/MP-NH<sub>2</sub> complexes, and (c) St3-shRNA/MP-NH<sub>2</sub> vs. St3-shRNA/PEI at 48 h (\* $p < 0.001$ ).

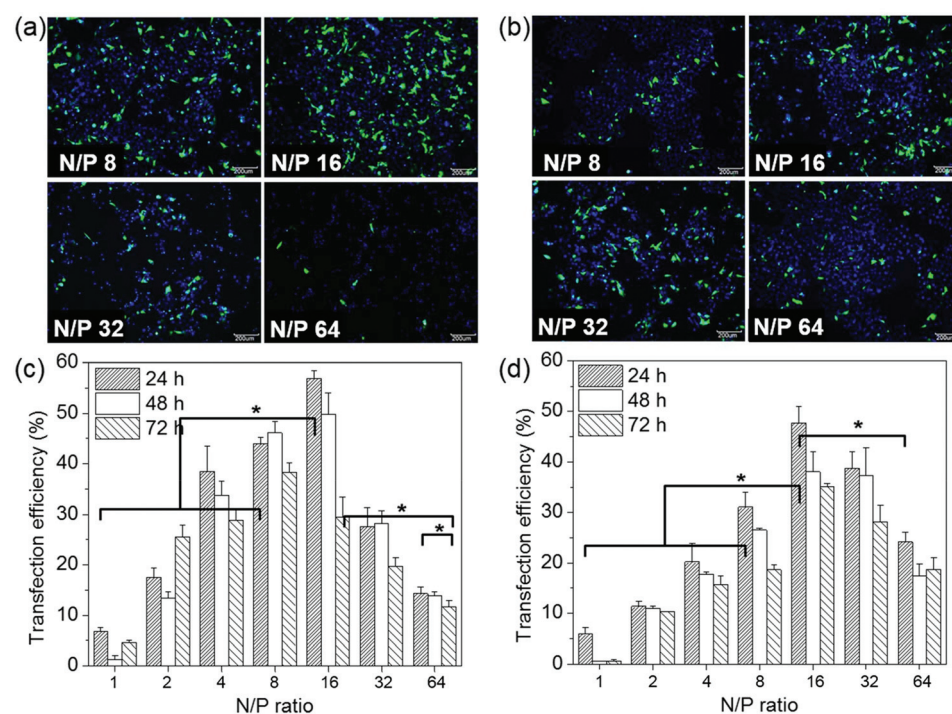


**Fig. 6** (a and b) Fluorescence images of B16F10 cancer cell after treatment with (a) St3-shRNA/PEI and (b) St3-shRNA/MP-NH<sub>2</sub> complexes (magnification,  $\times 100$ ; scale bar, 200  $\mu\text{m}$ ). (c and d) Transfection efficiencies after treatment with (c) St3-shRNA/PEI and (d) St3-shRNA/MP-NH<sub>2</sub> complexes were determined by FACAS at 24 h, 48 h, and 72 h (\* $p < 0.01$ ).

little fluorescence at the N/P charge ratio of 1, indicating low transfection efficiency. However, the transfection efficiency increased as N/P charge ratios increased and reached the maximum value at the N/P charge ratio of 16. Thereafter, a reduction in transfection efficiency was observed.

The transfection efficiencies of St3-shRNA/PEI were ~20%, ~30%, and ~50% at N/P charge ratios of 2, 4, and 16, respectively. As N/P charge ratios increased to 32 and 64 and the incubation time increased from 24 h to 72 h, St3-shRNA/PEI showed drastic decrease in transfection efficiency, probably due to the cytotoxicity of PEI.

Meanwhile, the transfection efficiencies of St3-shRNA/MP-NH<sub>2</sub> were ~10%, ~20%, and ~45% at N/P charge ratios of 2, 4, and 16

respectively. St3-shRNA/MP-NH<sub>2</sub> showed approximately 10% lower transfection efficiency than St3-shRNA/PEI. However, St3-shRNA/MP-NH<sub>2</sub> showed transfection efficiencies of 30% and 25% at N/P charge ratios of 32 and 64, respectively. Above the N/P charge ratio of 32, St3-shRNA/MP-NH<sub>2</sub> showed higher transfection efficiencies of approximately 10% than St3-shRNA/PEI. This indicated that St3-shRNA/MP-NH<sub>2</sub> complexes with N/P charge ratios of above 32 had lower cytotoxicity to B16F10 cancer cells and returned high transfection efficiencies, as expected.

### 3.5. Intratumoral injection of St3-shRNA/MP-NH<sub>2</sub> complexes

First, St3-shRNA/MP-NH<sub>2</sub> complexes were loaded in MP-NH<sub>2</sub> as an intratumoral injectable formulation. St3-shRNA/MP-NH<sub>2</sub>

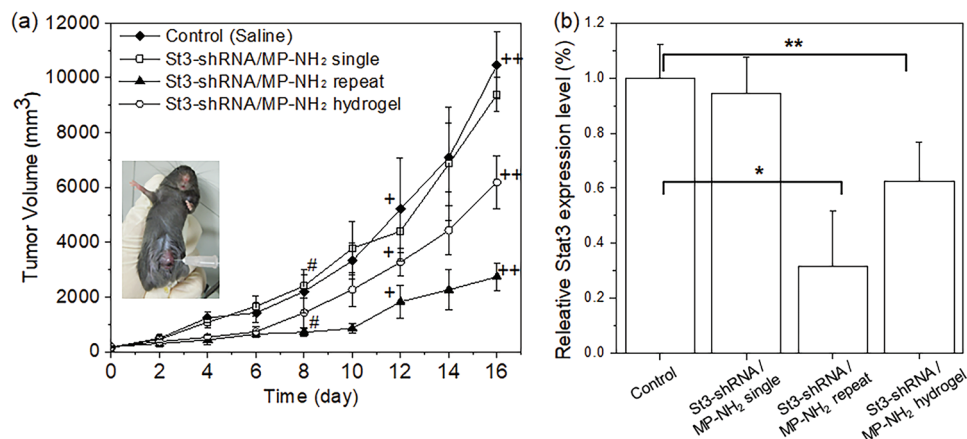


**Fig. 7** (a) Tumor volume (for 16 days) and (b) relative Stat3 expression level in B16F10 tumor (at 16 days) of xenograft-bearing mice injected with saline, single and repeat St3-shRNA/MP-NH<sub>2</sub> complexes, and single of St3-shRNA/MP-NH<sub>2</sub> complex-loaded hydrogels [(a)  $p < 0.01$  vs. the control group at 8 [#], 12 [+], and 16 [++]; and (b) \*  $p < 0.05$ , \*\*  $p < 0.01$ ].

complex-loaded hydrogel formulation flowed at 25 °C and became hydrogel at 37 °C, indicating its feasibility as an *in situ* forming hydrogel gene depot formulation for intratumoral injection. Next, formulations of saline, single injection of St3-shRNA/MP-NH<sub>2</sub> complexes, repeated injections of St3-shRNA/MP-NH<sub>2</sub> complexes, and St3-shRNA/MP-NH<sub>2</sub> complex-loaded hydrogel were prepared for *in vivo* intratumoral injections. Each formulation was injected directly into the tumor of xenografted animals (Fig. 7a).

Antiproliferative activities of formulations were assessed by monitoring changes in the tumor volume. The average tumor size on day 0 was  $165 \pm 14$  mm<sup>3</sup>. The change in tumor volume was monitored for 16 days after intratumoral injection to determine tumor volume doubling times and tumor growth rates (Table 1 and Fig. S1†).

Injections of saline and single injection of St3-shRNA/MP-NH<sub>2</sub> complexes (50 µg per mouse) resulted in very short doubling times of 2.8 days and 2.9 days and a rapid tumor growth rate of  $\sim 473$  mm<sup>3</sup> and 452 mm<sup>3</sup> per day, respectively.

Meanwhile, repeated injections of St3-shRNA/MP-NH<sub>2</sub> complexes extended the doubling time to 5.8 days and decreased the tumor growth rate to 126 mm<sup>3</sup> per day. Particularly, repeated injections of St3-shRNA/MP-NH<sub>2</sub> complexes highly suppressed tumor growth because St3-shRNA (50 µg per mouse) was injected repeatedly at 3, 6, 9, 12, and 15 days.

Meanwhile, single injection of St3-shRNA/MP-NH<sub>2</sub> complex-loaded hydrogel (50 µg per mouse) showed marginally

higher antitumor activity than single injection of only St3-shRNA/MP-NH<sub>2</sub> complexes. The antitumor activity of St3-shRNA/MP-NH<sub>2</sub> complex-loaded hydrogel was approximately the median value of the values obtained with single and repeated injections of St3-shRNA/MP-NH<sub>2</sub>. Even though St3-shRNA/MP-NH<sub>2</sub> complex-loaded hydrogel was injected once, these values may be justified by the sustained St3-shRNA release due to the hydrogel acting as a gene depot for St3-shRNA.

At 16 days, the Stat3 expression in the removed tumor tissue was examined to confirm the effect of Stat3 knockdown through the delivered St3-shRNA (Fig. 7b). Tumor tissues of mice administered a single injection of St3-shRNA/MP-NH<sub>2</sub> complexes showed low expression inhibition of 5% Stat3 knockdown compared to controls. However, 68% of Stat3 knockdown was observed in tumor tissues repeatedly that were administered St3-shRNA/MP-NH<sub>2</sub> complexes. Meanwhile, 38% of Stat3 knockdown was observed in St3-shRNA/MP-NH<sub>2</sub> complex-loaded hydrogel samples.

This implies that St3-shRNA delivered through St3-shRNA/MP-NH<sub>2</sub> complexes and St3-shRNA/MP-NH<sub>2</sub> complex-loaded hydrogel caused Stat3 knockdown and then reduced cancer cell proliferation and survival. Although repeated injections of St3-shRNA/MP-NH<sub>2</sub> complex resulted in higher Stat3 knockdown than single injections of St3-shRNA/MP-NH<sub>2</sub> complex-loaded hydrogel, we confirmed the effect of Stat3 knockdown with MP-NH<sub>2</sub> hydrogel acting as a gene depot for St3-shRNA.

**Table 1** Tumor volume doubling times and tumor growth rate after intratumoral injection

	Control	St3-shRNA/MP-NH <sub>2</sub> single	St3-shRNA/MP-NH <sub>2</sub> repeat	St3-shRNA/MP-NH <sub>2</sub> complex-loaded hydrogel
Tumor volume doubling time (days)	$2.8 \pm 1.5$	$2.9 \pm 1.4$	$5.8 \pm 1.9^b$	$3.7 \pm 2.0$
Tumor growth rate (mm <sup>3</sup> per day)	$472.8 \pm 314.3$	$451.6 \pm 282.3$	$125.5 \pm 81.3^a$	$342.9 \pm 182.9$

<sup>a</sup>  $p < 0.01$ . <sup>b</sup>  $p < 0.05$  vs. control at the same time-point.

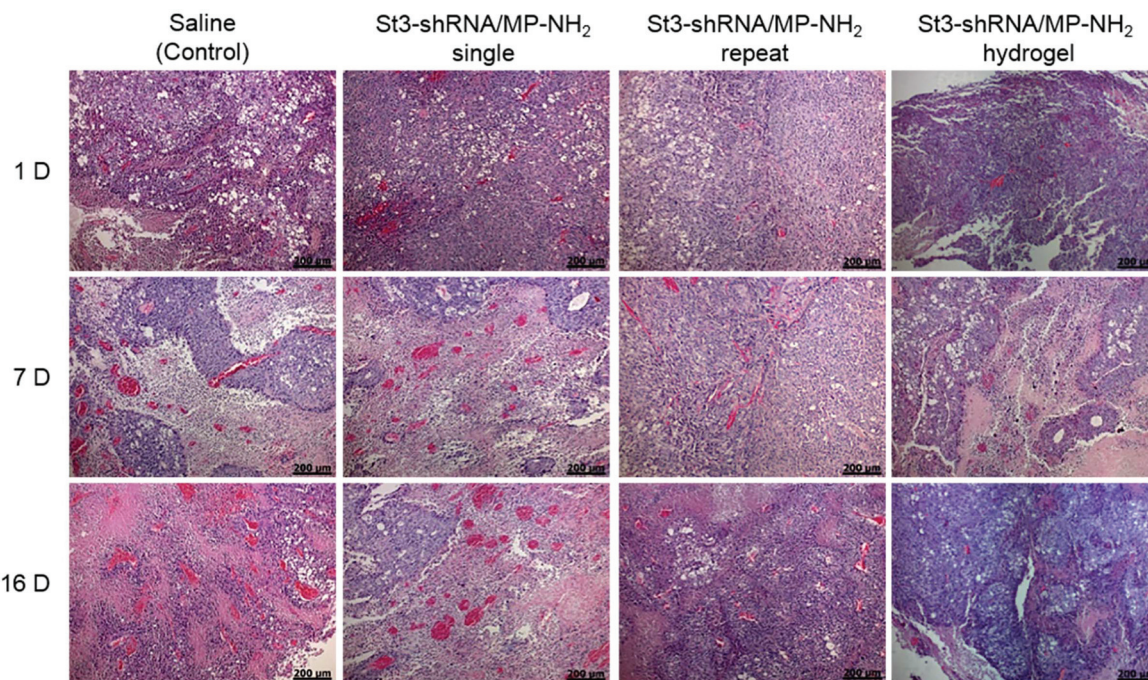


**Fig. 8** H&E-stained histological sections of tumors on days 1, 7, and 16 after intratumoral injection of xenograft-bearing mice with saline, St3-shRNA/MP-NH<sub>2</sub> complexes (single and repeat), and St3-shRNA/MP-NH<sub>2</sub> complex-loaded hydrogel (single) (scale bar = 200  $\mu$ m).

### 3.6. Histology studies

Histological sections of tumors injected with saline, St3-shRNA/MP-NH<sub>2</sub> complexes (single and repeat), and St3-shRNA/MP-NH<sub>2</sub> complex-loaded hydrogel (single) on days 1, 7, and 16 were examined after staining with H&E (Fig. 8). Immediately after intratumoral injection of saline, there was little necrosis and apparent blood vessels. The number of blood vessels increased as the implantation time increased.

Tumors that were injected with St3-shRNA/MP-NH<sub>2</sub> complexes only once showed a few regions with some degree of necrotic indices compared to saline-treated tumors. This implies that St3-shRNA/MP-NH<sub>2</sub> complexes can exhibit some antitumor activity at day 1. However, many blood vessels were observed and increased as the implantation time increased.

Tumors repeatedly injected with St3-shRNA/MP-NH<sub>2</sub> complexes and injected only once using St3-shRNA/MP-NH<sub>2</sub> complex-loaded hydrogel showed higher necrosis at day 1. The necrotic regions that were interspersed between areas of viable tumor increased as implantation time increased. Meanwhile, blood vessels were observed in tumors repeatedly administered using St3-shRNA/MP-NH<sub>2</sub> complexes or injected once using St3-shRNA/MP-NH<sub>2</sub> complex-loaded hydrogel.

The TUNEL staining showed the image of blue DAPI blue fluorescence (nuclei) and red TUNEL fluorescence (apoptosis) for tumors injected with saline, St3-shRNA/MP-NH<sub>2</sub> complexes (single and repeat), and St3-shRNA/MP-NH<sub>2</sub> complex-loaded hydrogel (single) after 1, 7, and 16 days (Fig. 9a). In tumors injected with saline, bright blue fluorescence, corresponding

to the nuclei of live cells was evident, and red fluorescence from TUNEL staining which represents apoptotic cells was absent. For tumors treated with a single injection of St3-shRNA/MP-NH<sub>2</sub> complexes, red TUNEL fluorescence was present at day 1 and then disappeared at day 7.

Meanwhile, for tumors treated with repeat injection of St3-shRNA/MP-NH<sub>2</sub> complexes, red TUNEL fluorescence attributable to apoptotic cells was observed. Additionally, this fluorescence gradually increased as the implantation time increased, indicating tumor cell apoptosis induced by the injected St3-shRNA/MP-NH<sub>2</sub> complexes. The tumors treated with St3-shRNA/MP-NH<sub>2</sub> complex-loaded hydrogel showed distinct red fluorescence due to tumor cell apoptosis at day 1, and the increased red fluorescence indicated large numbers of apoptotic cells at day 7. However, this fluorescence decreased day 16 onward.

TUNEL-positive cells were counted and normalized to the total stained tissue area to determine the extent of apoptosis (Fig. 9b and Fig. S2†). The percentage of apoptotic cells (TUNEL-positive cells) in the groups that were once and repeatedly injected with St3-shRNA/MP-NH<sub>2</sub> complexes were 10% and 11% at day 1, respectively. At day 6, however, the former showed no apoptotic cells, whereas the latter showed 40% and 52% apoptotic cells at days 7 and 16, respectively. This is because the latter group received a larger dose of St3-shRNA than the former.

Meanwhile, regarding the single injections of St3-shRNA/MP-NH<sub>2</sub> complex-loaded hydrogel, the percentage of apoptotic cells was 20% at day 1, 29% at day 6, and 21% at day 16. We speculate that this reflects the sustained release of St3-shRNA

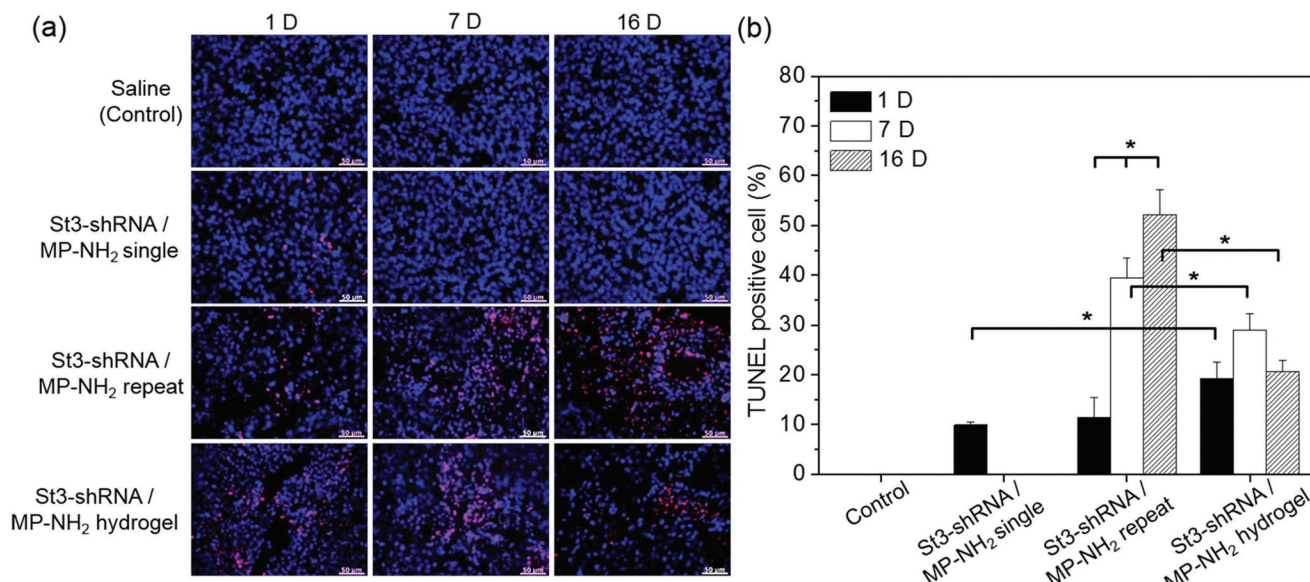


**Fig. 9** (a) Merged images of DAPI staining (blue: nuclei) and TUNEL staining (red: apoptotic cells) of tumors on days 1, 7, and 16 after intratumoral injection of xenograft-bearing mice with saline, St3-shRNA/MP-NH<sub>2</sub> complexes (single and repeat), and St3-shRNA/MP-NH<sub>2</sub> complex-loaded hydrogel (single) (scale bar = 50  $\mu$ m) and (b) number of TUNEL-positive cells on images (\* $p$  < 0.05).

from MP-NH<sub>2</sub> gene depot of St3-shRNA formed in the intratumorally injected tumor site and is thus able to achieve the sustained action periods of Stat3 knockdown.

This finding indicates that repeatedly delivering St3-shRNA through St3-shRNA/MP-NH<sub>2</sub> complexes and single delivery of St3-shRNA/MP-NH<sub>2</sub> complex-loaded hydrogel caused Stat3 knockdown and then increased apoptosis in tumor cells; among the two, the former showed better Stat3 knockdown effect owing to injection of a large dose of St3-shRNA.

## 4. Conclusion

Collectively, we successfully prepared MP-NH<sub>2</sub> with a cationic spermine segment as the gene carrier, a PEG segment to increase the stability of the complexes, and an amphiphilic segment for the formation of intratumoral *in situ* forming hydrogel gene depot. The intratumorally injected MP-NH<sub>2</sub> hydrogel St3-shRNA depot showed effective anti-tumor effect for an extended period of time due to the effect of Stat3 knockdown. The present findings showed that MP-NH<sub>2</sub> as the carrier and depot of St3-shRNA can provide a new strategy for St3-shRNA therapy through intratumoral injection with high efficacy and minimal adverse effects. The strategy of intratumoral St3-shRNA gene therapy using injectable *in situ* forming MP-NH<sub>2</sub> gene depot can provide a rationale for reducing the toxicity, increasing the efficacy and convenience in cancer patients.

## Funding

This study was supported by the National Research Foundation of Korea (NRF) grants, Creative Materials

Discovery Program (2019M3D1A1078938) and Priority Research Centers Program (2019R1A6A1A11051471).

## Author contributions

Conceptualization, D.Y.K. and M.S.K.; formal analysis, D.Y.K., H.J.J. and J.H.K.; funding acquisition, S.C. and M.S.K.; methodology, D.Y.K., H.J.J., J.H.K. and M.S.K.; project administration, S.C. and M.S.K.; supervision, S.C. and M.S.K.; validation, D.Y.K., H.J.J. and M.S.K.; visualization, D.Y.K. and H.J.J.; writing-original draft, D.Y.K.; writing-review and editing, M.S.K. All authors have read and agreed to the published version of the manuscript.

## Conflicts of interest

The authors declare no conflict of interest.

## References

- 1 J. Huynh, A. Chand, D. Gough and M. Ernst, *Nat. Rev. Cancer*, 2019, **19**, 82.
- 2 L. B. Ivashkiv, *Nat. Rev. Immunol.*, 2018, **18**, 545.
- 3 T. Fujimura, T. Fujimoto, A. Itaya-Hironaka, T. Miyaoka, K. Yoshimoto, S. Sakuramoto-Tsuchida, A. Yamauchi, M. Takeda, H. Tsujinaka, Y. Tanaka and S. Takasawa, *Clin. Rev. Allergy Immunol.*, 2017, **52**, 351.
- 4 B. R. A. Blechacz, R. L. Smoot, S. F. Bronk, N. W. Werneburg, A. E. Sirica and G. J. Gores, *Hepatology*, 2009, **50**, 1861.

- 5 K. Kaygisiz and C. V. Synatschke, *Biomater. Sci.*, 2020, **8**, 6113.
- 6 J. Kokkinos, R. M. C. Ignacio, G. Sharbeen, C. Boyer, E. Gonzales-Aloy, D. Goldstein, J. A. McCarroll and P. A. Phillips, *Biomaterials*, 2020, **240**, 119742.
- 7 Y. K. Bae, G. Kim, J. H. Kwon, M. Kim, S. J. Choi, W. Oh, S. Um and H. J. Jin, *Tissue Eng. Regener. Med.*, 2020, **17**, 193.
- 8 S. Bhattacharjee, B. Roche and R. A. Martienssen, *RNA Biol.*, 2019, **16**, 1133.
- 9 Z. Wen, F. Liu, Q. Chen, Y. Xu, H. Li and S. Sun, *Biomater. Sci.*, 2019, **7**, 4414.
- 10 R. Acharya, *Mater. Sci. Eng., C*, 2019, **104**, 109928.
- 11 R. L. Setten, J. J. Rossi and S. P. Han, *Nat. Rev. Drug Discovery*, 2019, **18**, 421.
- 12 D. Chouhan, N. Dey, N. Bhardwaj and B. B. Mandal, *Biomaterials*, 2019, **216**, 11926.
- 13 H. Wang, S. Ding, Z. Zhang, L. Wang and Y. You, *J. Gene Med.*, 2019, **21**, e3101.
- 14 R. S. Bora, D. Gupta, T. K. S. Mukkur and K. S. Saini, *Mol. Med. Rep.*, 2012, **6**, 9.
- 15 L. Johannes and M. Lucchino, *Nucleic Acid Ther.*, 2018, **28**, 178.
- 16 Z. Xu, D. Wang, Y. Cheng, M. Yang and L. P. Wu, *Mater. Sci. Eng., C*, 2018, **92**, 1006.
- 17 W. Zhong, X. Li, J. L. Pathak, L. Chen, W. Cao, M. Zhu, Q. Luo, A. Wu, Y. Chen, L. Yi, M. Ma and Q. Zhang, *Biomater. Sci.*, 2020, **8**, 3664–3677.
- 18 M. Kullberg, R. McCarthy and T. J. Anchordoquy, *J. Controlled Release*, 2013, **172**, 730–736.
- 19 A. Hoffman, *Adv. Drug Delivery Rev.*, 1998, **33**, 185.
- 20 D. Scherman, A. Rousseau, P. Bigey and V. Escriou, *Gene Ther.*, 2017, **24**, 151.
- 21 B. Ozpolat, A. K. Sood and G. Lopez-Berestein, *Adv. Drug Delivery Rev.*, 2014, **66**, 110.
- 22 H. Elzeny, F. Zhang, E. N. Ali, H. A. Fathi, S. Zhang, R. Li, M. A. El-Mokhtar, M. A. Hamad, K. L. Wooley and M. Elsabahy, *Drug Des., Dev. Ther.*, 2017, **11**, 483.
- 23 O. D. Mrowczynski, S. T. Langan and E. Rizk, *Clin. Neurol. Neurosurg.*, 2018, **166**, 124.
- 24 M. Devarasetty, S. D. Forsythe, E. Shelkey and S. Soker, *Tissue Eng. Regener. Med.*, 2020, **17**, 759.
- 25 S. H. Park, J. Y. Seo, J. Y. Park, Y. B. Ji, K. Kim, H. S. Choi, S. Choi, J. H. Kim, B. H. Min and M. S. Kim, *NPG Asia Mater.*, 2019, **11**, 30.
- 26 H. Y. Seo, D. Y. Kim, D. Y. Kwon, J. S. Kwon, L. M. Jin, B. Lee, J. H. Kim, B. H. Min and M. S. Kim, *Biomaterials*, 2013, **34**, 2748.
- 27 H. J. Kim, S. J. You, D. H. Yang, H. J. Chun and M. S. Kim, *J. Ind. Eng. Chem.*, 2020, **84**, 226.
- 28 M. G. Kim, T. W. Kang, J. Y. Park, S. H. Park, Y. B. Ji, H. J. Ju, D. Y. Kwon, Y. S. Kim, S. W. Kim, B. Lee, H. S. Choi, H. B. Lee, J. H. Kim, B. Y. Lee, B. H. Min and M. S. Kim, *Mater. Sci. Eng., C*, 2019, **103**, 109853.
- 29 B. K. Lee, J. H. Noh, J. H. Park, S. H. Park, J. H. Kim, S. H. Oh and M. S. Kim, *Tissue Eng. Regener. Med.*, 2018, **15**, 393.
- 30 J. H. Park, S. H. Park, H. Y. Lee, J. W. Lee, B. K. Lee, B. Y. Lee, J. H. Kim and M. S. Kim, *Biomaterials*, 2018, **154**, 86.
- 31 D. Y. Kim, D. Y. Kwon, J. S. Kwon, J. H. Kim, B. H. Min and M. S. Kim, *Polym. Rev.*, 2015, **55**, 407–452.
- 32 J. I. Kim, D. Y. Kim, D. Y. Kwon, H. J. Kang, J. H. Kim, B. H. Min and M. S. Kim, *Biomaterials*, 2012, **33**, 2823.
- 33 J. H. Park, H. J. Kang, D. Y. Kwon, B. K. Lee, B. Lee, J. W. Jang, H. J. Chun, J. H. Kim and M. S. Kim, *J. Mater. Chem. B*, 2015, **3**, 8143.
- 34 S. H. Kim, J. H. Park, J. S. Kwon, J. G. Cho, K. G. Park, C. H. Park, J. J. Yoo, A. Atala, H. S. Choi, M. S. Kim and S. J. Lee, *Biomaterials*, 2020, **258**, 120267.
- 35 M. S. Kim, H. H. Ahn, Y. N. Shin, M. H. Cho, G. Khang and H. B. Lee, *Biomaterials*, 2007, **28**, 5137.
- 36 Y. Xu, C. S. Kim, D. M. Saylor and D. Koo, *J. Biomed. Mater. Res., Part B*, 2017, **105**, 1692.
- 37 S. A. Salem, Z. Rashidbenam, M. H. Jasman, C. C. K. Ho, I. Sagap, R. Singh, M. R. Yusof, Z. M. Zainuddin, R. B. H. Idrus and M. H. Ng, *Tissue Eng. Regener. Med.*, 2020, **17**, 553.
- 38 M. Igartua, R. M. Hernández, A. Esquisabel, A. R. Gascón, M. B. Calvo and J. L. Pedraz, *J. Controlled Release*, 1998, **56**, 63.
- 39 R. Allen, E. Ivchenko, B. Thuamsang, R. Sangsuwan and J. S. Lewis, *Biomater. Sci.*, 2020, **8**, 6056–6068.
- 40 J. H. Lee, H. B. Lee and J. D. Andrade, *Prog. Polym. Sci.*, 1995, **20**, 1043–1079.